

Article

Wideband UHF Antenna for Partial Discharge Detection

Zhen Cui ¹, Seungyong Park ¹, Hosung Choo ²  and Kyung-Young Jung ^{1,*} 

¹ Department of Electronics Computer Engineering, Hanyang University, Seoul 04763, Korea; czblaze@hanyang.ac.kr (Z.C.); seungyong@hanyang.ac.kr (S.P.)

² School of Electronic and Electrical Engineering, Hongik University, Seoul 04066, Korea; hschoo@hongik.ac.kr

* Correspondence: kyjung3@hanyang.ac.kr; Tel.: +82-2-2220-2320

Received: 29 January 2020; Accepted: 27 February 2020; Published: 2 March 2020



Abstract: This paper presents a ultra-high frequency (UHF) antenna for partial discharge (PD) detection and the antenna sensor can be used near a conducting ground wire. The proposed UHF antenna has advantages of easy setup and higher-frequency detection over the high-frequency current transformer (HFCT) sensor. First, a variety of loop-shaped antennas are designed to compare each near field coupling capability. Then, a new UHF antenna is designed based on the loop-shaped antenna, which has the best near field coupling capability. Finally, the proposed UHF antenna is fabricated and measured. It provides a wide impedance bandwidth of 760 MHz (740–1500 MHz). Its simple setup configuration and wide bandwidth frequency response in the UHF band can provide a more efficient means for PD detection.

Keywords: partial discharge; ultra-high frequency (UHF) antenna

1. Introduction

With the significant increase in electric power consumption, power equipment is currently being developed towards large capacity, ultra-high voltage, and unmanned control. If such large capacity power equipment fails to work, in general, it takes considerable time to repair the entire system and resume electric power supply. Among many factors that cause the failure in the power equipment, partial discharge (PD), which is a localized discharge in an electrical dielectric insulation system under high-voltage (HV) field, is the major cause of power equipment failure. Power plant accidents are closely related to the dielectric breakdown in HV power equipment, and thus there has been increasing demand for real-time PD diagnostics for HV power equipment [1,2]. There are several techniques for detecting the PD, including optical, acoustic, electrical, and electromagnetic (EM) wave detection methods [3]. Among them, the electromagnetic wave detection method is widely used due to its high detection sensitivity and robust anti-interference ability [4].

Therefore, high frequency (HF) and ultra-high frequency (UHF) sensors have popularly been studied in PD detection systems. PD events in HV power equipment typically produce very short current pulses with a rise time of less than 1 nanosecond, which can emit EM waves in the GHz frequency band [5]. When this PD occurs, the UHF sensor detects the EM waves emitted by the PD [6], so the UHF antenna is a core part of the UHF PD detection system, and the performance of the UHF antenna can directly affect the detection performance of the system [7–12]. There are two approaches to detect the PD in the EM wave detection method. One is to install a PD sensor on the surface of the metallic chassis of HV power equipment for directly detecting the PD inside HV power equipment. The other is to place the PD sensor near a conducting ground wire for detecting the PD current flowing through the wire. Figure 1 shows a PD detection approach using a high-frequency current transformer (HFCT), which is one of the common techniques for detecting the PD currents

on the conducting ground wire. When the HFCT is applied to the PD detection system of HV power equipment, the HFCT should completely surround the conducting ground wire with various shapes and sizes, which increases the complexity and inconvenience of the experiment [13].

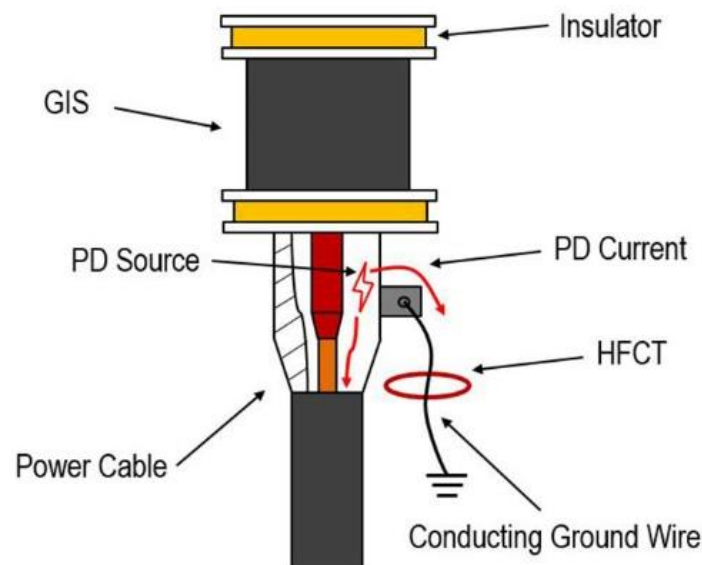


Figure 1. Partial discharge (PD) detection mechanism using the high-frequency current transformer (HFCT).

In this work, a novel UHF antenna is designed to detect the PD in HV power equipment, which is placed nearby the conducting ground wire, rather than completely surrounding the conducting wire as shown in the conceptual diagram of Figure 2. Herein, the PD detection can be easily implemented since it does not need to be clamped to the conducting ground wire, different from the HFCT. In addition, the proposed UHF antenna can detect the PD signals in the conducting ground wire in the GHz frequency band that exceeds the detection range of the HFCT.

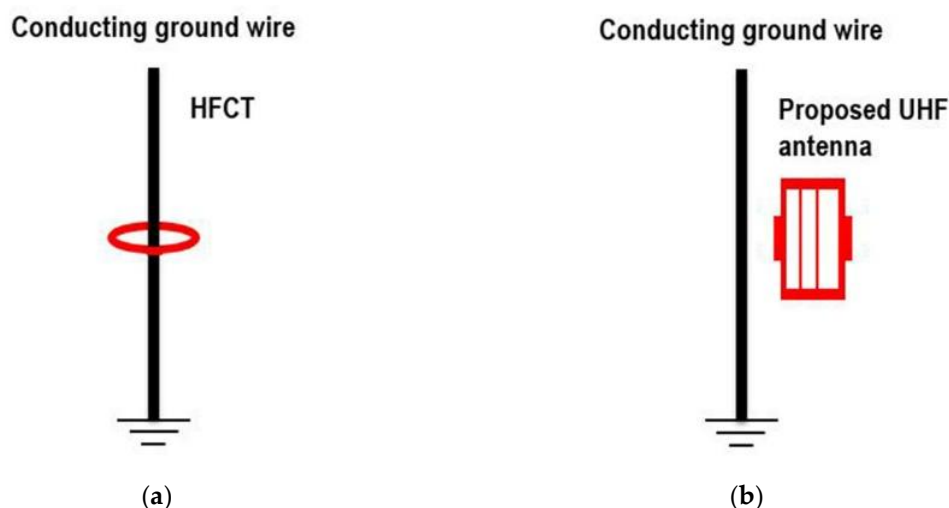


Figure 2. Conceptual diagram for the PD detection in the conducting ground wire: (a) HFCT and (b) proposed ultra-high frequency (UHF) antenna.

First, various shapes of loop antennas are examined to compare their near field coupling capabilities. Through the preliminary parametric study, a novel UHF antenna is proposed based on the basic loop antenna structure, which has the best near field coupling capability. The proposed UHF antenna is then fabricated, and the PD detection performance is measured using the experimental setup that can

imitate the conducting ground wire of the HV power equipment. Experimental results demonstrate that the proposed UHF antenna can effectively detect the PD currents.

2. Basic Loop Antenna

As alluded previously, we will design a loop-shaped antenna suitable for PD detection in the conducting ground wire. Toward this purpose, we considered various shaped loop antennas, including circle, square, rectangle, rhombic, and elliptical loop antennas [14–19]. Since we investigated the UHF antenna for PD detection from 500 –1500 MHz, various simple loop antennas were designed at 1 GHz, the center frequency of the operating band. In other words, the total circumference was approximately 300 mm, one wavelength at the frequency. In order to choose a proper loop-shaped antenna, we investigated the detection capabilities of various antennas mentioned above. The current source was injected into the conducting ground wire, and the coupling performance of the loop antennas was calculated by the ratio of the received voltage (at the antenna port) to the injected current (into the conducting ground wire). The distance between the injected current source and the plane of the antenna is d , as shown in the simulation models in Figure 3. The voltages received at the loop antennas were calculated by integrating the electric field in the antenna port using the HFSS field calculator function [20] as follows:

$$V = \int \mathbf{E} \cdot d\mathbf{l}$$

where \mathbf{E} is the electric field in the antenna port and $d\mathbf{l}$ indicates the differential displacement along a line in the antenna port. As shown in Figure 4, rectangle #1 yields the best performance.

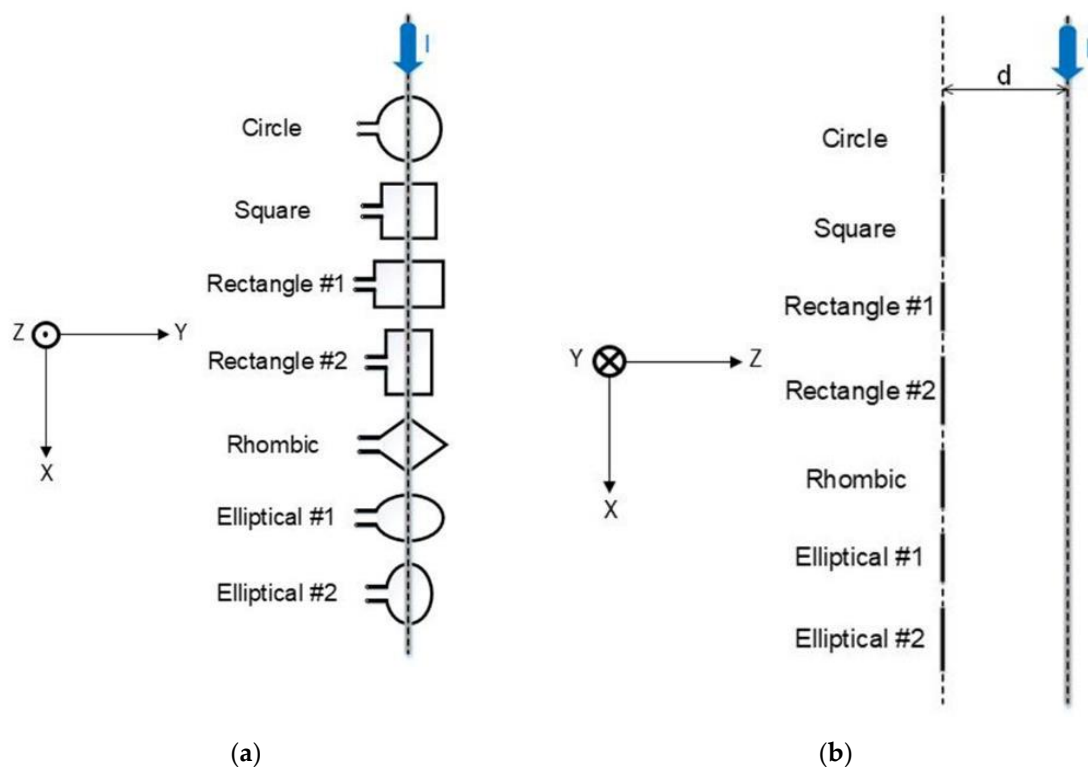


Figure 3. Simulation models of loop antennas: (a) top view and (b) side view.

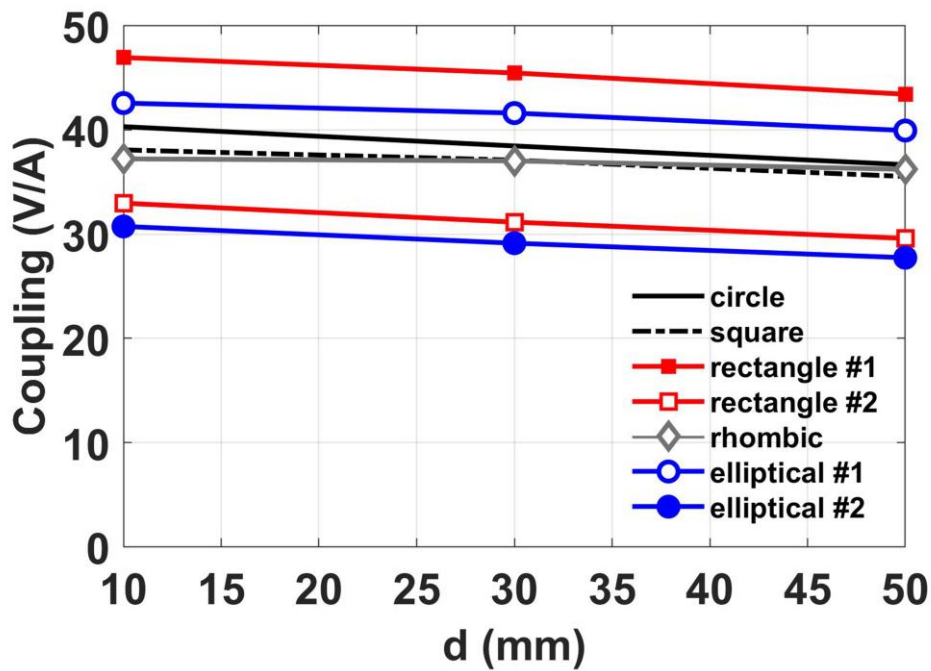


Figure 4. Coupling performance of each antenna.

The spectral response of coupling performance for rectangle #1 was also investigated in Figure 5. As d increased, the coupling performance decreased, especially for shorter wavelengths. Note that the reduction of the received voltage was negligible as the distance increase since the distance difference was very small compared to the wavelength. The simulation results show that the rectangle #1 antenna could have a good ability to sense the near field, but the bandwidth of this basic loop antenna was narrow. In the next section, we focused on increasing the operating bandwidth of the antenna.

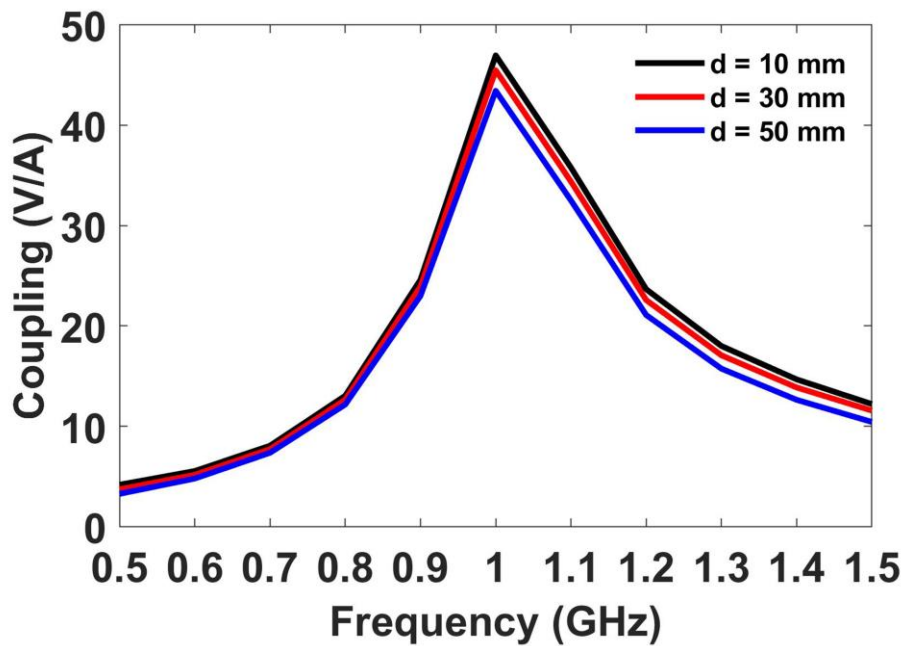


Figure 5. Coupling performance by rectangle #1 versus frequency.

3. Wideband Ultra-High Frequency (UHF) Antenna

The bandwidth of the basic loop antenna is extremely narrow because of its resonant structure, as mentioned in the previous section. In this work, in order to enhance the bandwidth of the antenna, the rectangle #1 loop antenna was modified.

To increase the bandwidth, first, we designed the antenna (modified antenna 1 in Figure 6b) on the FR4 (a relative permittivity of 4.4, a thickness of 1.6 mm, and a loss tangent of 0.02) and changed the position of the feed line. It is worth noting that the employment of FR4 could lead to size reduction and the variation of the feeding point could lead to a change in the return loss. In specific, the antenna could have two resonance points at 0.7 GHz and 1.29 GHz, as shown in Figure 7a. However, the antenna matching performance was still not good, especially at the center frequency. Therefore, the antenna was further modified by adding two stubs (modified antenna 2 in Figure 6c). This antenna could increase the effective electrical length and improve the antenna impedance matching from 0.76 to 1.2 GHz. However, S_{11} was still greater than -10 dB in the range of 0.93–1.10 GHz. In order to tackle this issue, the strip width of the antenna was increased to further improve the antenna impedance matching. The final design of the proposed antenna was performed by using HFSS optimization. The S_{11} parameters and the smith charts of the step-by-step design antennas are shown in Figure 7. As shown in the figures, S_{11} parameters got lower and loci were located further into the center of the smith chart as the antenna design evolved. Note that the final antenna could have $S_{11} < -10$ dB from 0.71 to 1.5 GHz.

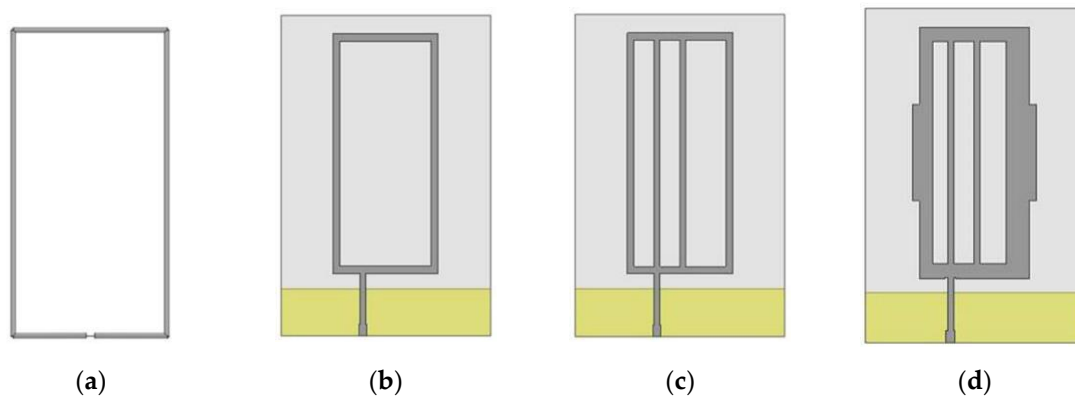


Figure 6. The geometry of loop antennas: (a) basic loop antenna; (b) modified antenna 1; (c) modified antenna 2; and (d) final antenna.

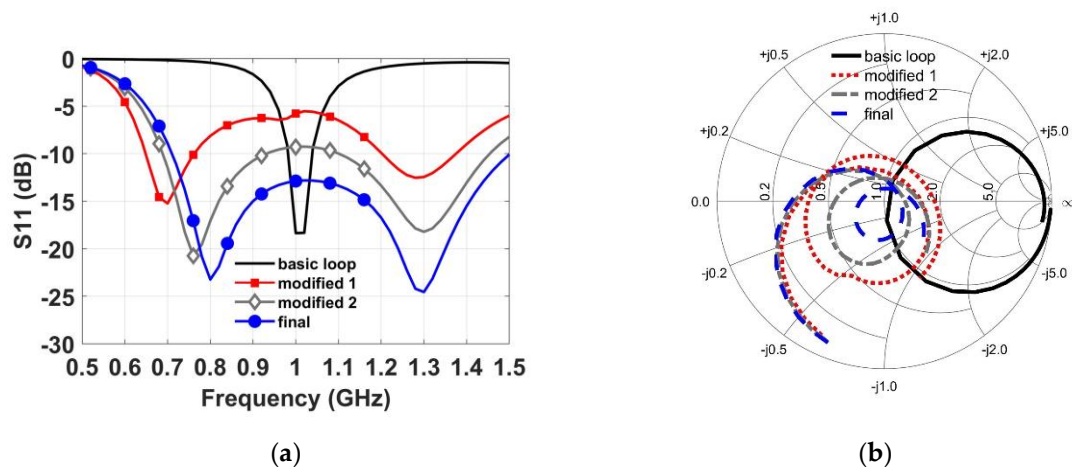


Figure 7. Antenna matching performance: (a) S_{11} parameters. (b) Smith chart.

The geometry of the final UHF antenna is shown in Figure 8 and the design parameters of the proposed antenna are listed in Table 1. Figure 9 shows that the real part of the impedance was near 50 ohm and the imaginary part of the impedance was near 0 ohm in the range of 710–1500 MHz. It indicates that the antenna had good impedance matching in the frequency range of interests.

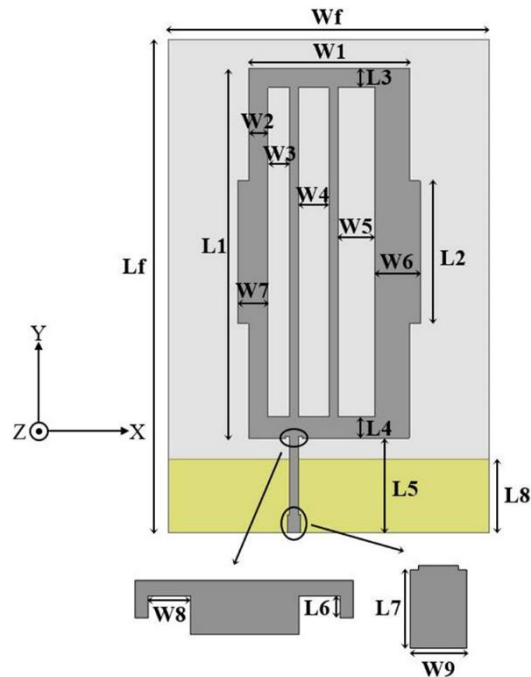


Figure 8. The geometry of the proposed UHF antenna.

Table 1. Design parameters of the proposed UHF antenna.

Parameters	Value (mm)	Parameters	Value (mm)
Lf	138	W1	45
Wf	89.5	W2	5.5
L1	103.5	W3	6
L2	40	W4	8.5
L3	5.5	W5	10.5
L4	6	W6	12.5
L5	26.5	W7	8.5
L6	0.5	W8	1
L7	5	W9	3.5
L8	20.5		

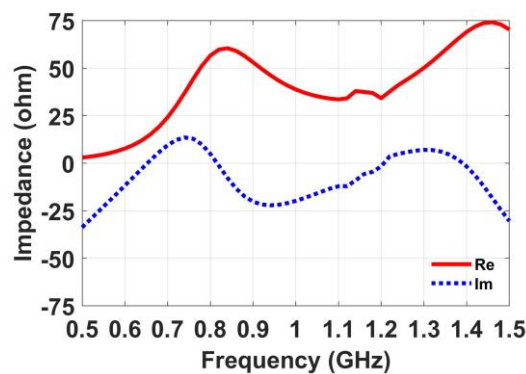


Figure 9. Input impedance of the proposed UHF antenna.

4. Fabrication and Measured Results

The proposed UHF antenna was printed on a FR4 substrate with the dimensions of $89.5 \text{ mm} \times 138 \text{ mm} \times 1.6 \text{ mm}$, and the photograph of the fabricated antenna is shown in Figure 10. The S_{11} of the antenna was measured in an anechoic chamber ($W = 3 \text{ m}$, $L = 6 \text{ m}$, and $H = 3 \text{ m}$) using a vector network analyzer (Agilent Technologies E5071C). Figure 11 depicts the simulated and measured S_{11} parameters of the proposed antenna. It is shown that S_{11} was less than -10 dB from 740 to 1500 MHz . The measurement result agreed well with the simulation result. Slight discrepancies between the simulation and measurement could be caused by fabrication and measurement errors.

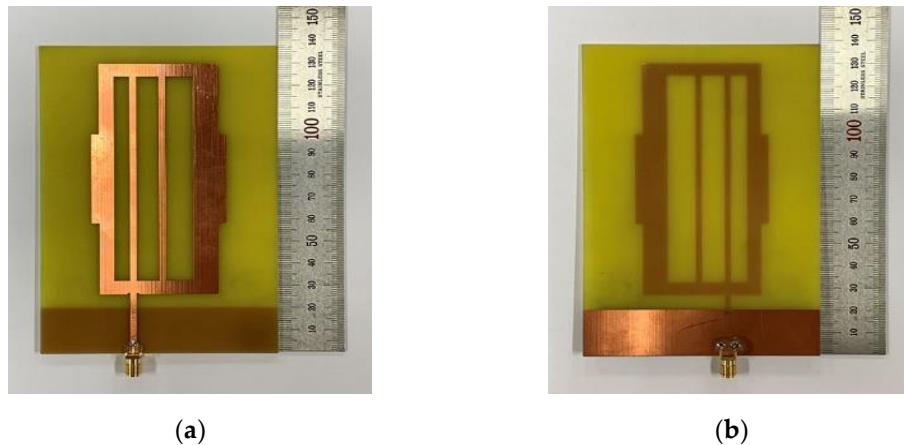


Figure 10. The prototype of the proposed UHF antenna: (a) top view and (b) bottom view.

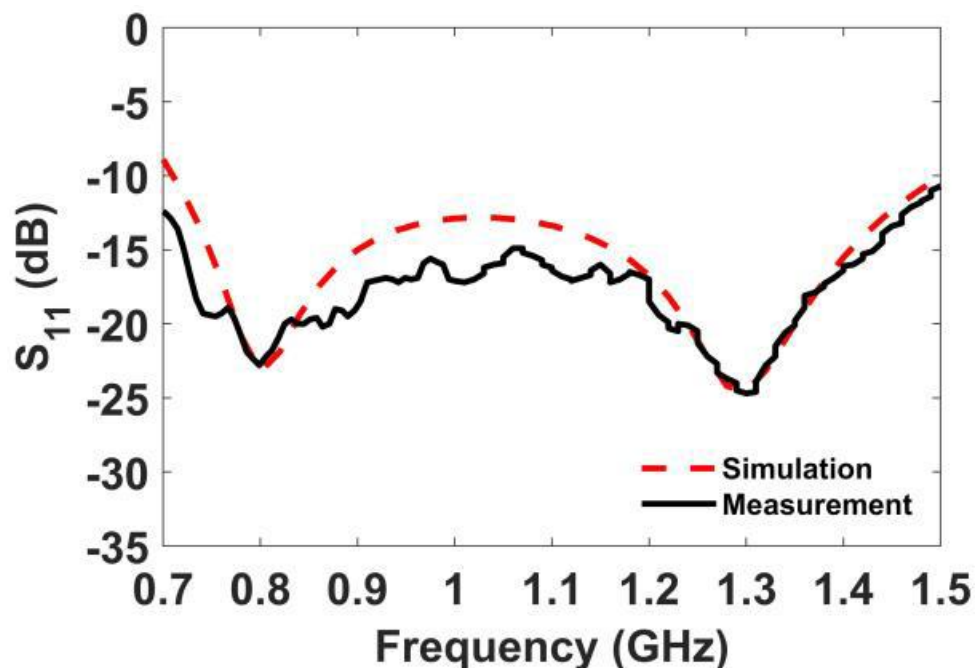


Figure 11. Simulation and measurement results (S_{11}) of the proposed UHF antenna.

In order to estimate the PD detection ability, we set up a test system in our laboratory, as shown in Figure 12. We used a RG316 coaxial cable to imitate the conducting ground wire of the HV power equipment. Toward this purpose, the protective dielectric layer and the metal net in the middle of the coaxial line were peeled off so that the EM waves could be emitted to the outside. At the end of the coaxial cable, we connected a 50 ohm termination to imitate the wire that is grounded to the earth. The other end of the coaxial cable was connected to port 1 of the vector network analyzer. The fabricated

antenna was placed below the center of the coaxial cable, same as Figure 3. The SMA connector of the antenna was connected to port 2 of the vector network analyzer. The PD detection ability could be inferred by the S_{21} parameter. Note the test system employed in this work was not exactly same as the previous simulation in Section 2 because there were discontinuities of the peeled coaxial cable. Nonetheless, the test setup in our work could obtain the trends of the coupling performance since the S_{21} parameter was proportional to the coupling coefficient of Section 2.

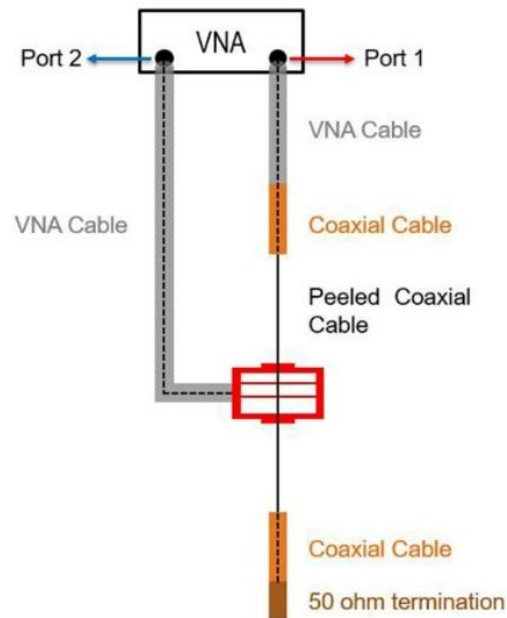


Figure 12. PD experimental set-up for the antenna test.

We investigated the S_{21} parameters for the different distances (10 mm, 20 mm, and 30 mm) between the peeled coaxial cable and the antenna. Figure 13 shows the actual measurement picture for the distance of 10 mm. As shown in Figure 13, the 10 mm-thick Styrofoam was placed under the ends of the coaxial cable and fixed with tape, which made the coaxial cable to be firmly placed 10 mm above the antenna. Note that more Styrofoam was stacked for the tests with longer distances. As shown in Figure 14, the S_{21} parameters lay between -10 and -40 dB in both simulation and measurement results. Discrepancies between the measurement results and simulation results might be caused by fabrication and measurement errors including antenna misalignment, the non-perfectly straight peeled coaxial cable, etc. It should be noted that it would be useful to provide a exact methodology to extract the coupling coefficient of Section 2 using the available measurement equipment. In future work, this extraction methodology should be addressed and studied.

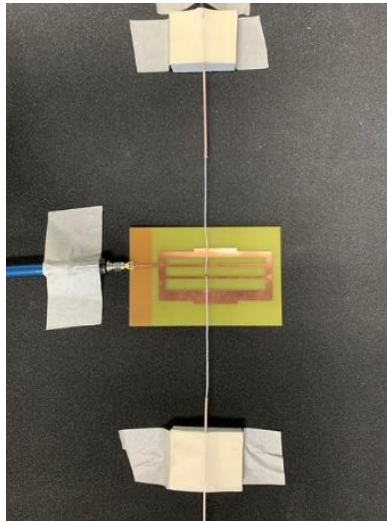


Figure 13. Actual measurement picture.

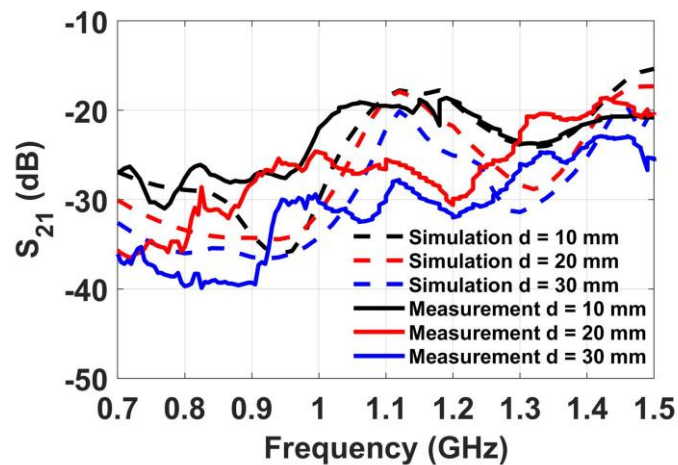


Figure 14. Simulation and measurement results (S_{21}).

5. Conclusions

In this work, a wideband UHF antenna for PD detection was proposed. This antenna could provide a wide bandwidth of 760 MHz (740–1500 MHz). The proposed antenna was an offset structure to the conducting ground wires so that it did not have to be clamped to the conducting ground wires to detect PD. Such a simple structure makes it easy to carry and use for the PD detection system of HV power equipment nearby conducting ground wires. The proposed UHF antenna can be used for PD detection on conducting ground wires in any power equipment systems such as electric vehicles.

Author Contributions: The presented work was carried out in collaboration of all authors. Z.C. performed the simulations. S.P., H.C. and K.-Y.J. participated to the conception, fabrication and experiment. Z.C. wrote the paper, which was edited by all co-authors. All authors have read and agreed to the published version of the manuscript.

Funding: This research was funded by Basic Science Research Program through the National Research Foundation of Korea (NRF) funded by the Ministry of Education (No. 2015R1A6A1A03031833 and No. 2017R1D1A1B03034537).

Conflicts of Interest: The authors declare no conflict of interest.

References

1. Wang, M.; Vandermaar, A.J.; Srivastava, K.D. Review of condition assessment of power transformers in service. *IEEE Electr. Insul. Mag.* **2002**, *18*, 12–25. [[CrossRef](#)]
2. Ha, S.-G.; Cho, J.; Lee, J.; Min, B.-W.; Choi, J.; Jung, K.-Y. Numerical study of estimating the arrival time of UHF signals for partial discharge localization in a power transformer. *J. Electromagn. Eng. Sci.* **2018**, *18*, 94–100. [[CrossRef](#)]
3. Soomro, I.A.; Ramdon, M.N. Study on different techniques of partial discharge (PD) detection in power transformers winding: Simulation between paper and EPOXY resin using UHF method. *Int. J. Concept. Electr. Electron. Eng.* **2014**, *2*, 57–61.
4. Judd, M.D.; Yang, L.; Hunter, I.B.B. Partial discharge monitoring of power transformers using UHF sensors part 1: Sensors and signal interpretation. *IEEE Electr. Insul. Mag.* **2005**, *21*, 5–14. [[CrossRef](#)]
5. Chai, H.; Phung, B.T.; Zhang, D. Development of UHF sensors for partial discharge detection in power transformer. In Proceedings of the 2018 Condition Monitoring and Diagnosis (CMD), Perth, Australia, 1–5 September 2018.
6. Yang, F.; Peng, C.; Yang, Q.; Luo, H.; Ullah, I.; Yang, Y. An UWB printed antenna for partial discharge UHF detection in high voltage switchgears. *Prog. Electromagn. Res. C* **2016**, *69*, 105–114. [[CrossRef](#)]
7. Sinaga, H.H.; Phung, B.T.; Blackburn, T.R. Partial discharge localization in transformers using UHF detection method. *IEEE Trans. Dielectr. Electr. Insul.* **2012**, *19*, 1891–1900. [[CrossRef](#)]
8. Jahangir, H.; Akbari, A.; Werle, P.; Akbari, M.; Szczechowski, J. UHF characteristics of different types of PD sources in power transformers. In Proceedings of the Iranian Conference on Electrical Engineering (ICEE), Tehran, Iran, 2–4 May 2017; pp. 1242–1247.
9. Rozi, F.; Khayam, U. Development of loop antennas for partial discharge detection. *Int. J. Electr. Eng. Inform.* **2015**, *7*, 29–41. [[CrossRef](#)]
10. Li, J.; Jiang, T.; Wang, C.; Cheng, C. Optimization of UHF Hilbert Antenna for Partial discharge detection of transformers. *IEEE Trans. Antennas Propag.* **2012**, *60*, 2536–2540.
11. Muslim, J.; Khayam, S.U.; Hikita, M. Enhanced bowtie UHF antenna for detecting partial discharge in gas insulated substation. In Proceedings of the 48th International Universities' Power Engineering Conference (UPEC), Dublin, Ireland, 2–5 September 2013.
12. Khosronejad, M.; Gentili, G.G. Design of an Archimedean spiral UHF antenna for pulse monitoring application. In Proceedings of the 2015 Loughborough Antennas & Propagation Conference (LAPC), Loughborough, UK, 2–3 November 2015.
13. Alvarez, F.; Garnacho, F.; Ortego, J.; Sanchez-Uran, M.A. Application of HFCT and UHF sensors in on-line partial discharge measurements for insulation diagnosis of high voltage equipment. *Sensors* **2015**, *15*, 7360–7387. [[CrossRef](#)] [[PubMed](#)]
14. Balanis, C.A. *Antenna Theory: Analysis and Design*, 3rd ed.; John Wiley & Sons, Inc: New Jersey, NJ, USA, 2005.
15. Hur, J.; Byun, G.; Choo, H. Design of small CRPA arrays with circular microstrip loops for electromagnetically coupled feed. *J. Electromagn. Eng. Sci.* **2018**, *18*, 129–135. [[CrossRef](#)]
16. O, Y.; Jin, Y.; Choi, J. A compact four-port coplanar antenna based on an excitation switching reconfigurable mechanism for cognitive radio applications. *Appl. Sci.* **2019**, *9*, 3157. [[CrossRef](#)]
17. Samanta, G.; Mitra, D. Dual-band circular polarized flexible implantable antenna using reactive impedance substrate. *IEEE Trans. Antennas Propag.* **2019**, *67*, 4218–4223. [[CrossRef](#)]
18. Lee, H.; Zahid, Z.; Kim, H. Loop-Type ground radiation antenna for a C-Shaped ground plane. *J. Electromagn. Eng. Sci.* **2019**, *19*, 1–5. [[CrossRef](#)]
19. Sung, Y. Dual-band circularly polarized stack-ring antenna. *J. Electromagn. Eng. Sci.* **2019**, *19*, 37–41. [[CrossRef](#)]
20. Available online: <http://www.ansys.com/products/electronics/ansys-hfss> (accessed on 30 July 2019).

